Voltage Response of Primary Resonance of Electrostatically Actuated MEMS Clamped Circular Plate Resonators

Dumitru I. Caruntu[1]
Mem. ASME
Department of Mechanical Engineering,
University of Texas Rio Grande Valley,
1201 W University Drive,
Edinburg, TX 78539
e-mails: dumitru.caruntu@utrgv.edu;
caruntud2@asme.org

Reynaldo Oyervides
Department of Mechanical Engineering,
University of Texas Rio Grande Valley,
1201 W University Drive,
Edinburg, TX 78539
e-mail: reynaldo64@hotmail.com

This paper investigates the voltage–amplitude response of soft alternating current (AC) electrostatically actuated micro-electro-mechanical system (MEMS) clamped circular plates for sensing applications. The case of soft AC voltage of frequency near half natural frequency of the plate is considered. Soft AC produces small to very small amplitudes away from resonance zones. Nearness to half natural frequency results in primary resonance of the system, which is investigated using the method of multiple scales (MMS) and numerical simulations using reduced order model (ROM) of seven terms (modes of vibration). The system is assumed to be weakly nonlinear. Pull-in instability of the voltage–amplitude response and the effects of detuning frequency and damping on the response are reported. [DOI: 10.1115/1.4033252]

Introduction

MEMS are used in automotive industry and medical field [1], as microswitches, transistors, sensors, micromirrors, microgrippers, microvalves, resonators [2], resonator sensors [3], and actuators for mechanical stimulation of living cells [4]. Electrostatic actuation is preferred due to low energy consumption of operation and high precision with which they can be controlled [5,6]. Other forms of actuation are piezoelectric and magneto-electric. Most MEMS device structures include elements such as cantilevers, bridges, and plates of different shapes and boundary conditions.

A large class of electrostatically actuated MEMS structure consists of flexible cantilevers, bridges, or plates suspended above a parallel, rigid ground plate. A direct current (DC) voltage applied between the flexible beam/plate and the fixed ground plate produces an attracting electrostatic force between them. The flexible plate deforms toward the ground plate into a new equilibrium position [7] where electrostatic and elastic forces balance each other. The elastic restoring force within the flexible plate opposes deformation. AC voltage is used on top of the DC voltage to cause the system to vibrate around this equilibrium position. Such systems are called resonators [6–8]. If the electrostatic force overcomes the elastic restoring force, the system becomes unstable and the flexible plate collapses onto the ground plate in a phenomenon known as the pull-in instability. The voltage at which this instability phenomenon occurs is known as the pull-in voltage [7]. Electrostatically actuated MEMS response depends on voltage and frequency of actuation, and initial displacement and velocity of the plate.

Due to the high cost and time consumption of experimentation, extensive research has been done to accurately model and simulate these systems mathematically. These models can be used to predict pull-in instability and the pull-in voltage [9,10]. Investigations have been conducted for MEMS devices such as clamped–clamped microbeams at primary, superharmonic, and subharmonic resonances [7,11]. These structures may experience hardening or softening effects depending on the excitation voltages and frequencies used [7].

Amplitude frequency response is widely used to investigate the behavior of MEMS resonators. This type of response explains how the steady-state amplitude of vibration of the system changes with the excitation frequency while the voltage is kept constant [8,10,12]. Bifurcation points in the frequency response give the frequencies at which the stability of the system changes from stable to unstable and vice versa. Amplitude frequency responses are used to predict the changes in stability, pull-in, and hardening or softening effects. The behavior of circular plates under axisymmetric vibration was investigated [13] using the MMS to obtain the amplitude frequency response of the system and show that circular plates may undergo internal resonance due to interactions between the mode of vibration at certain frequencies. Investigations using MMS and ROM method to obtain the amplitude frequency response of other structures such as cantilever resonators were reported in the literature [6,8,14,15].

Voltage–amplitude response is important for MEMS resonators. This response predicts the change in stability due to change in voltage. A continuous model of the pull-in effect in electrostatically actuated MEMS circular plates, limited to DC voltage, has been reported [16]. The static pull-in, i.e., the DC voltage is gradually increased until the center of the plate deflection leads to pull-in, and dynamic pull-in, i.e., the DC voltage is applied to the undeformed plate producing a rapid deflection leading to pull-in, have been investigated. Another model [17] of electrostatically actuated circular microplates, limited to DC voltage actuation, based on von Karman's nonlinear bending theory, and including Casimir force, was used to investigate pull-in instability and vibration of prestressed microplates. Specifically, using the shooting method, the static deformation and the pull-in parameters, and the small amplitude free vibration about predeformed bending position, were reported. A simplified model of elasto-electrostatic analysis of thin circular microplates used as ultrasonic transducers [18] was used to predict the pull-in DC voltage. The electrostatic force was expanded in Taylor series and terms up to the squared term were retained, and then the Galerkin-weighted residual technique was used for predictions. The results were in agreement with ANSYS simulations. A similar study [19] reported the pull-in voltage and free vibrations of functionally graded material circular microplate subjected to DC voltage and mechanical shock. The effect of surface stress on the pull-in instability [20] of electrostatically actuated circular nanoplates subjected to DC voltage and hydrostatic pressure was reported. It has been found that the surface stress effect is more significant in the pull-in of lower thickness nanoplates. Size-dependent behavior of capacitive circular microplates [21] was reported as well. Using Hamilton's

[1]Corresponding author.

Contributed by the Design Engineering Division of ASME for publication in the JOURNAL OF COMPUTATIONAL AND NONLINEAR DYNAMICS. Manuscript received January 31, 2015; final manuscript received March 22, 2016; published online May 13, 2016. Assoc. Editor: Daniel J. Segalman.

principle, the static and dynamic pull-in of microplates under DC voltage were investigated. It has been found that the intrinsic size dependence of materials has an effect on both pull-in voltage and natural frequency. A review of electrostatic pull-in instability can be found in the literature [22].

ROM [23] was used to investigate the effects of voltage on the natural frequencies of clamped circular plates. Caruntu et al. [5] investigated the voltage response of electrostatically actuated MEMS cantilever resonators. The actuation consisted of soft AC voltage of frequency near half natural frequency of the structure. "Soft AC is the voltage that produces soft electrostatic forces in the system, i.e., it produces small to very small amplitudes (with respect to the gap between the resonator and the ground plate) when the frequency is away from resonance zones" [24]. Two methods, ROM and MMS were used to numerically simulate the behavior of the system.

This paper investigates the voltage–amplitude response of electrostatically actuated clamped circular plates undergoing axisymmetric vibrations under soft AC voltage of frequency near half natural frequency of the plate. This results in primary resonance of the system as showed afterward. This investigation is conducted using MMS and two integration methods of ROM; one uses AUTO 07, a software package for continuation and bifurcation problems, to obtain the voltage–amplitude response [25], and the other one uses MATLAB to obtain time responses of the structure.

To the best of our knowledge, this is the first time when (1) the voltage response of primary resonance of electrostatically actuated MEMS circular plates (a distributed-parameter model) subjected to soft AC voltage actuation is reported, (2) using two methods of investigation, namely MMS and ROM, in which (3) a convergence investigation of the ROM is conducted. (4) A good agreement between MMS and ROM is shown for gap-amplitudes (amplitudes with respect to the gap) less than 0.5. It is also shown that for large gap-amplitudes, up to pull-in (contact between the resonator and the ground plate), (5) only seven terms (vibration modes) ROM can accurately predict the behavior of the resonator; MMS fails in this range. (6) The effects of frequency and damping on the voltage response are reported.

Differential Equation of Motion

The system involves a deformable MEMS circular plate clamped around its edges and suspended above a rigid ground plate as shown in Fig. 1. R is the outer radius of the uniform circular plate, d is the gap between the plates, and w is the dimensionless deflection of the plate. Dimensional equation of axisymmetric vibrations of electrostatically actuated circular plates [26] is given by

$$\rho h\frac{\partial^2\hat{u}}{\partial\hat{t}^2}+2c_1\frac{\partial\hat{u}}{\partial\hat{t}}+D\left(\frac{\partial^4\hat{u}}{\partial\hat{r}^4}+\frac{2}{r}\frac{\partial^3\hat{u}}{\partial\hat{r}^3}-\frac{1}{\hat{r}^2}\frac{\partial^2\hat{u}}{\partial\hat{r}^2}+\frac{1}{\hat{r}^3}\frac{\partial\hat{u}}{\partial\hat{r}}\right)=\frac{\varepsilon^*V^2}{2(d-\hat{u})^2} \tag{1}$$

At the right hand side of Eq. (1) is the electrostatic force [2]. The variables of Eq. (1) are: $\hat{t}$, time; $\hat{r}$, radial coordinate; and $\hat{u}(t,r)$, dimensional deflection of the plate. The MEMS plate constants and parameters are: ε^*, electrical permittivity; ρ, density; h, thickness; $2c_1$, damping coefficient; V, voltage; and $D=Eh^3/[12(1-\nu^2)]$ plate flexural rigidity, where E is Young modulus and ν the Poisson's ratio. Constants and typical dimensional MEMS plate characteristics used in this investigation were obtained from the literature [16,27], and are shown in Tables 1 and 2. The voltage is assumed to be AC voltage, i.e., $V=V_0\cos\Omega\hat{t}$, where V_0 is the amplitude and Ω the circular frequency of the voltage.

The resulting dimensionless equation of motion for circular plates under electrostatic actuation undergoing axisymmetric vibrations is given by

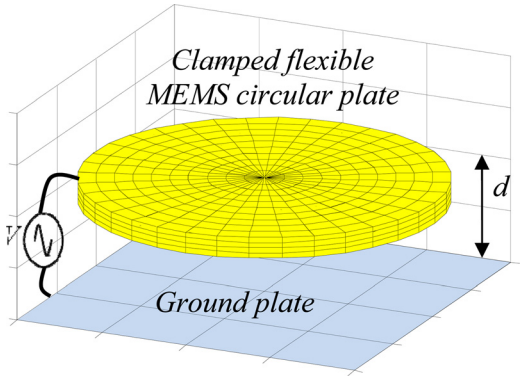

Fig. 1 MEMS uniform clamped circular plate of radius *R* and thickness *h* suspended above ground plate at a gap distance *d*

$$\frac{\partial^2u}{\partial t^2}+\mu\frac{\partial u}{\partial t}+\frac{\partial^4u}{\partial r^4}+\frac{2}{r}\frac{\partial^3u}{\partial r^3}-\frac{1}{r^2}\frac{\partial^2u}{\partial r^2}+\frac{1}{r^3}\frac{\partial u}{\partial r}=\frac{\delta\cos^2\Omega^*t}{(1-u)^2} \tag{2}$$

where the corresponding dimensionless variables t, r, $u(t,r)$ are as follows:

$$t=\hat{t}\sqrt{\frac{D}{\rho hR^4}},\quad r=\frac{\hat{r}}{R},\quad u=\frac{\hat{u}}{d} \tag{3}$$

The dimensionless μ damping parameter, δ dimensionless voltage parameter, and Ω^* dimensionless excitation frequency are given by

$$\mu=2c_1\sqrt{\frac{R^4}{\rho hD}},\quad \delta=\frac{R^4\varepsilon^*V_0^2}{2Dd^3},\quad \Omega^*=\Omega\sqrt{\frac{\rho hR^4}{D}} \tag{4}$$

Using Tables 1 and 2, the dimensionless parameters μ and δ are shown in Table 3.

Method of Multiple Scales

The first approach to investigate the behavior of the electrostatically actuated clamped circular plates is using MMS which is a perturbation method. MMS allows for investigating the voltage response, i.e., the relationship between the amplitude of vibration and the applied AC voltage, for various frequencies. In what follows, only soft actuation and weak damping are considered since MMS is valid only for weakly nonlinear systems, i.e., systems for which although the nonlinear effects play an essential role, the linear terms are dominant. MMS transforms the nonlinear differential equation modeling MEMS into a system of linear differential equations. Two scales are considered for this model, namely, the fast scale $T_0=t$ and the slow scale $T_1=\varepsilon t$. In order to use MMS, the electrostatic force of Eq. (2) must be expanded in Taylor series. The dimensionless partial differential equation of motion becomes

$$\frac{\partial^2u}{\partial t^2}+\varepsilon\mu\frac{\partial u}{\partial t}+P[u]=\varepsilon\delta(1+2u+3u^2+4u^3)\cos^2(\Omega t) \tag{5}$$

where the operator P is given by

Table 1 System constants [16]

Young's modulus	E	150.6	GPa
Poisson's ratio [27]	ν	0.23	
Material density	ρ	2330.0	kg/m^3
Space permittivity	ε^*	8.854×10^{-12}	C^2/N·m^2

Table 2 Dimensional system characteristics [16]

Radius of plate	R	250.0	μm
Initial gap distance	d	1.014	μm
Plate thickness	h	3.01	μm
Damping	c_1	2.014	N·s/m^3
Voltage	V_0	1.044	V

$$P = \left[\frac{\partial^4}{\partial r^4} + \frac{2}{r}\frac{\partial^3}{\partial r^3} - \frac{1}{r^2}\frac{\partial^2}{\partial r^2} + \frac{1}{r^3}\frac{\partial}{\partial r}\right] \tag{6}$$

and the small dimensionless bookkeeping device parameter ε [28–30] is used to scale the assumed weakly nonlinear electrostatic force and damping. Consider a first-order uniform MMS expansion of the deflection as follows:

$$u = u_0 + \varepsilon u_1 \tag{7}$$

where u_0 and u_1 are components of the solution to be found. The partial derivative with respect to time, using the fast and slow timescales, becomes

$$\frac{\partial}{\partial t} = D_0 + \varepsilon D_1 \ , \quad D_0 = \frac{\partial}{\partial T_0} \ , \quad D_1 = \frac{\partial}{\partial T_1} \tag{8}$$

Since this investigation deals with the behavior of the circular plate under AC voltage of frequency near half the natural frequency ω_k, the excitation frequency Ω can be written as

$$\Omega = \frac{\omega_k}{2} + \varepsilon\sigma \tag{9}$$

where σ is frequency detuning parameter. Substituting Eqs. (7)–(9) into Eq. (5) results in

$$\begin{aligned}(D_0 + \varepsilon D_1)^2(u_0 + \varepsilon u_1) + P(u_0 + \varepsilon u_1) = -\varepsilon\mu(D_0 + \varepsilon D_1)(u_0 + \varepsilon u_1) \\ + \varepsilon\delta[1 + 2(u_0 + \varepsilon u_1) + 3(u_0 + \varepsilon u_1)^2 + 4(u_0 + \varepsilon u_1)^3] \\ \cos^2(\omega_k T_{0/2} + \sigma T_1)\end{aligned} \tag{10}$$

Equation (10) is expanded and then the terms including the coefficients ε^0 and ε^1 are collected resulting into zero-order and first-order problems as follows:

$$\varepsilon^0: \quad D_0^2 u_0 + P[u_0] = 0 \tag{11}$$

$$\begin{aligned}\varepsilon^1: D_0 u_1 + P(u_1) = -2D_0 D_1 u_0 - \mu D_0 u_0 \\ + \delta\left(1 + 2u_0 + 3u_0^2 + 4u_0^3\right)\cos^2\left(\frac{1}{2}\omega_k T_0 + \sigma T_1\right)\end{aligned} \tag{12}$$

The solution u_0 of Eq. (11) along with the boundary conditions for a clamped circular plate results as follows:

$$u_0 = \phi_k(r)[A(T_1)e^{i\omega_k T_0} + \overline{A}(T_1)e^{-i\omega_k T_0}] \tag{13}$$

where $\phi_k(r)$ are the mode shapes of vibration and ω_k the corresponding natural frequencies [31,32]. The complex conjugate coefficients $A(T_1)$ and $\overline{A}(T_1)$ of Eq. (13) are to be determined. The mode shapes of vibration for a circular plate are given by

Table 3 Dimensionless system parameters

Voltage parameter	δ	0.050
Damping parameter	μ	0.005

$$\phi_k(r) = \left(\frac{J_0\left(\sqrt{\omega_k}\cdot r\right)}{J_0\left(\sqrt{\omega_k}\right)} - \frac{I_0\left(\sqrt{\omega_k}\cdot r\right)}{I_0\left(\sqrt{\omega_k}\right)}\right) \tag{14}$$

where J_0, I_0 are Bessel functions of first kind and modified first kind, respectively. The first three mode shapes of axisymmetrical vibrations are shown in Fig. 2. The mode shapes are orthonormal [30], i.e., they satisfy $\int_0^1 r\phi_n(r)\phi_m(r)dr = \delta_{nm}$, where δ_{nm} is the Kronecker delta. The solution given by Eq. (13) is substituted into Eq. (12). Expanding the resulting equation, collecting the secular terms ($e^{i\omega_k T_0}$), and setting their sum equal to zero in order to eliminate them (the sum of the secular terms has to be zero for all T_0) leads to

$$\begin{aligned}-2i\omega_k\phi_k A' - \mu i\omega_k\phi_k A + \frac{1}{4}\delta e^{2i\sigma T_1} + \delta\phi_k A \\ + \frac{3}{4}\delta e^{-2i\sigma T_1}\phi_k^2 A^2 + \frac{3}{2}\delta e^{2i\sigma T_1}\phi_k^2 A\overline{A} + 6\delta\phi_k^3 A^2\overline{A} = 0\end{aligned} \tag{15}$$

where A' is the derivative of the complex amplitude A with respect to the slow timescale T_1. Solvability condition requires that Eq. (15) is orthogonal to any solution of the homogeneous equation. Therefore multiplying expression (15) by the operator given below

$$\int_0^1 \bullet r\phi_k(r)dr \tag{16}$$

results in

$$\begin{aligned}-2i\omega_k g_{k2}A' - \mu i\omega_k g_{k2}A + \frac{1}{4}\delta e^{2i\sigma T_1} g_{k1} + \delta A g_{k2} \\ + \frac{3}{4}\delta g_{k3} e^{-2i\sigma T_1}A^2 + \frac{3}{2}\delta g_{k3} e^{2i\sigma T_1}A\overline{A} + 6\delta g_{k4}A^2\overline{A} = 0\end{aligned} \tag{17}$$

where g_{kn} coefficients are as follows:

$$g_{kn} = \int_0^1 r\phi_k^n(r)dr, \quad n = 1,2,3,4 \tag{18}$$

The complex amplitudes A and $\overline{A}$ are written in exponential form as

$$A = \frac{1}{2}ae^{i\beta} \ \text{ and } \ \overline{A} = \frac{1}{2}ae^{-i\beta} \tag{19}$$

where a and β, the real amplitude and phase of the motion, are then replaced into Eq. (17). The subsequent equation is multiplied by $e^{-i\beta}$, and the real and the imaginary parts are then separated resulting into two first-order differential equations with the independent variable T_1 and the two dependent variables a and β. These equations are transformed into an autonomous system, i.e., one in which T_1 does not appear explicitly [30] by denoting

$$\gamma = 2\sigma T_1 - \beta \tag{20}$$

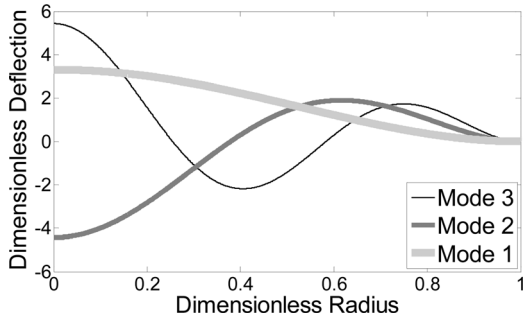

Fig. 2 First three mode shapes of vibration for clamped circular plates with $r = 0$ the center of plate, and $r = 1$ the edge

and substituting γ into these differential equations. The resulting differential equations are in terms of a and γ, where γ is the phase difference between the response of the structure and the actuation. The amplitude and phase are not changing at a singular point [30]; therefore, steady-state solutions result from $a' = \gamma' = 0$ and they are given by

$$a = \frac{4}{3}\frac{\mu\omega_0 g_{k2}}{\delta g_{k3}\sin\gamma} \pm \sqrt{\frac{16}{9}\frac{\mu^2\omega_0^2 g_{k2}^2}{\delta^2 g_{k3}^2\sin^2\gamma} - \frac{4}{3}\frac{g_{k1}}{g_{k3}}} \tag{21}$$

$$\sigma = \left(-\frac{1}{8}\frac{g_{k1}}{a} - \frac{9}{32}a g_{k3}\right)\frac{\delta\cos\gamma}{\omega_0 g_{k2}} - \frac{1}{4}\frac{\delta}{\omega_0} - \frac{3\delta a^2 g_{k4}}{8\omega_0 g_{k2}} \tag{22}$$

Using Eqs. (13), (19), and (20), and considering $\varepsilon = 1$, [28–30], one can find u_0 to include the dependence between nonlinear frequency and amplitude.

Reduced Order Model

The second method used in this research is a numerical method, namely, ROM. This method does not require assuming weak nonlinearities, but requires a certain number of terms (a convergence investigation needs to be conducted). In this work, the convergence investigation is showed in "Voltage–Amplitude Response" section. ROM can be used to accurately investigate both low amplitude and high amplitude vibrations. ROM is more accurate than MMS and gives a better understanding of the pull-in instability. The deflection at any point of the circular plate can be described by

$$u(r,t) = \sum_{i=1}^{N} u_i(t)\phi_i(r) \tag{23}$$

where the number of terms (modes of vibration) N of the ROM is finite, the dimensionless displacement u is a function of time-dependent functions $u_i(t)$ to be determined, and the mode shapes $\phi_i(r)$ are given by Eq. (14). The partial differential equation of motion Eq. (2) is multiplied by $(1-u^2)$ in order to eliminate all displacement terms from the denominator and reduce the computational cost [33]. Then Eq. (23) is substituted into the resulting equation which is next multiplied by the operator of Eq. (16) where $k = n$. The following system of equations results:

$$\begin{aligned}
&\sum_{i=1}^{N}\frac{\partial^2 u_i}{\partial t^2}\left(\int_0^1 r\phi_n\phi_i dr - 2\sum_{j=1}^{N}u_j\int_0^1 r\phi_n\phi_i\phi_j dr + \sum_{jk}^{N}u_j u_k\int_0^1 r\phi_n\phi_i\phi_j\phi_k dr\right)\\
&= -\mu\left(\sum_{i=1}^{N}\frac{\partial u_i}{\partial t}\int_0^1 r\phi_n\phi_i dr - 2\sum_{ij}^{N}\frac{\partial u_i}{\partial t}u_j\int_0^1 r\phi_n\phi_i\phi_j dr + \sum_{ijk}^{N}\frac{\partial u_i}{\partial t}u_j u_k\int_0^1 r\phi_n\phi_i\phi_j\phi_k dr\right)\\
&-\sum_{i=1}^{N}\omega_i^2 u_i\int_0^1 r\phi_n\phi_i dr + 2\sum_{ij}^{N}\omega_i^2 u_i u_j\int_0^1 r\phi_n\phi_i\phi_j dr - \sum_{ijk}^{N}\omega_i^2 u_i u_j u_k\int_0^1 r\phi_n\phi_i\phi_j\phi_k dr + \delta\int_0^1 r\phi_n dr\cos^2\Omega t
\end{aligned} \tag{24}$$

where $n = 1, 2, ..., N$. ROM is a Galerkin-based method [1]. Since this work investigates the behavior of the circular plate at half the natural frequency, the excitation frequency Ω is given by Eq. (8) for $\varepsilon = 1$ [28]. The resulting system of second-order differential equations (24) is transformed into a system of first-order differential equations and then integrated using AUTO 07 for $N = 2, 3, 4, 5, 6, 7$ terms in order to investigate the convergence of ROM and obtain the voltage response. Also, time responses are found for desired voltage and frequency using another software package, namely, MATLAB. Steady-state amplitudes of the center of the circular plates are then obtained. The voltage–amplitude response is used to understand the relationship between the amplitude of vibration and the applied AC voltage, as shown in the following section "Voltage-Amplitude Response". The effects of the detuning frequency, excitation voltage, and damping on the system are reported. ROM numerical results are compared to MMS analytical results in the next section "Voltage-Amplitude Response".

Voltage–Amplitude Response

Numerical simulations are conducted for the frequency of actuation near half of the fundamental natural frequency, i.e. k=1 in Eq. (9). The coefficients of Eq. (18) in this case are g_{11}=0.5155, g_{12}=1.0005, g_{13}=2.3381, and g_{14}=5.9763. System constants [16] from Eq. (4) are shown in Table 1. The dimensional system parameters of a typical circular microplate [16] used to conduct these simulations are shown in Table 2, and their corresponding dimensionless values are shown in Table 3. The first seven dimensionless natural frequencies of vibration of a clamped circular plate are shown in Table 4. The relationship between the dimensionless natural frequencies and the dimensional ones is the relationship in Eq. (4) between the dimensionless excitation frequency and the dimensional one. These natural frequencies are used to determine the first seven axisymmetric mode shapes of vibration, Eq. (14). The mode shapes obtained are then used to calculate the total displacement at the center of the circular plate as shown in Eq. (23). In this paper, soft electrostatic AC actuation is considered. The AC frequency is near half natural frequency of the circular plate, which results in a primary resonance phenomenon.

Figure 3 shows the amplitude–voltage response of seven terms reduced order model (7T-ROM) in comparison with MMS. This response is a bifurcation diagram. U_{max} is the amplitude of vibration of the center of the plate, and δ is the dimensionless voltage parameter used to excite the system while the detuning frequency σ is held constant. The steady-state solutions response shown consists of two branches, a stable branch shown as solid line, and unstable branch shown as dashed line. Starting from rest at equilibrium position, as the AC voltage is increased at constant frequency, the amplitude of vibration of the center of the plate increases until it reaches the saddle-node bifurcation point A,

Table 4 First seven dimensionless natural frequencies for clamped circular plate

	$N=1$	$N=2$	$N=3$	$N=4$	$N=5$	$N=6$	$N=7$
ω_k	10.216	39.771	89.104	158.183	247.005	355.568	483.872

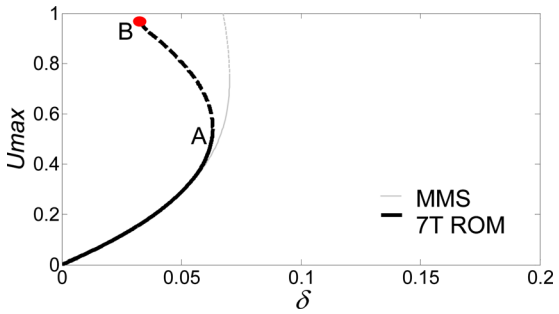

Fig. 3 Voltage response for MEMS clamped circular plate using MMS and seven terms ROM, $\mu = 0.005$, $\sigma = -0.005$

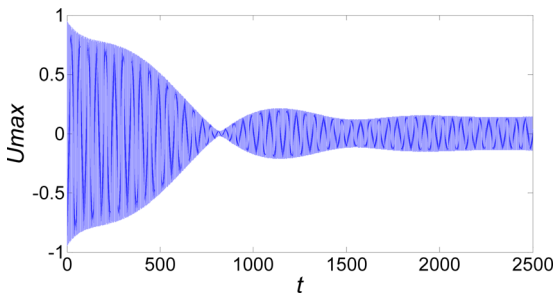

Fig. 4 Time response for MEMS clamped circular plate for 7T ROM, $\delta = 0.03$, $\mu = 0.005$, $\sigma = -0.005$, initial amplitude $U_0 = 0.95$

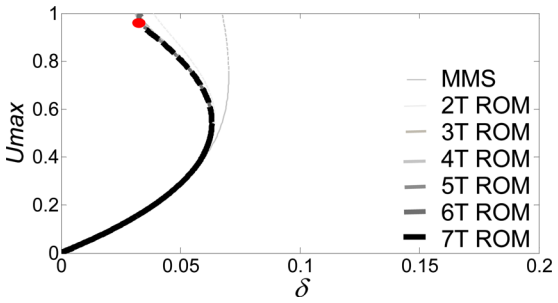

Fig. 6 Zoom-in view of high amplitudes of Fig. 6 convergence of ROMs, $\mu = 0.005$, $\sigma = -0.005$

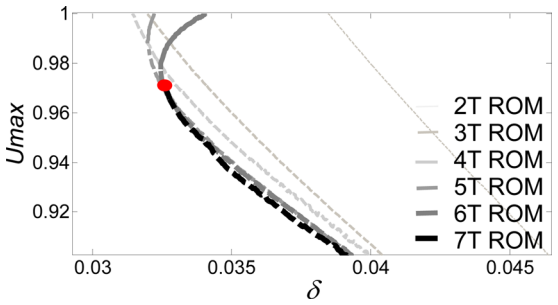

Fig. 7 Zoom on the convergence of ROM terms from Fig. 5, $\mu = 0.005$, $\sigma = -0.005$

where the system loses stability and jumps to $U_{\max} = 1$ which is pull-in (contact with the ground plate). The unstable solutions located on dashed branch are saddle points. In the voltage range of unstable branch, the amplitude decreases and settles to the corresponding (same voltage) low amplitude on the stable branch if the initial amplitude is below the dashed line, and increases to pull-in ($U_{\max} = 1$) if the initial amplitude is above the dashed line. The branch shown in gray is the response using MMS. As can be noticed, the response from using 7T ROM and MMS are in agreement for amplitudes below 0.4 of the gap. This is due to MMS being limited to weak nonlinearities, thus underestimating the nonlinear behavior of the system at high amplitudes. MMS fails to predict the saddle-node bifurcation point and the pull-in phenomenon for large initial amplitudes, above the unstable branch AB, which can occur due to disturbances such as mechanical shock [34,35] or spike of a undesired DC voltage acting on the structure.

Figures 4 and 5 show two time responses using 7T ROM MATLAB simulations in order to validate the AUTO results. Using an initial displacement $U_0 = 0.95$ of the gap for the voltage parameter $\delta = 0.03$, which is below the unstable branch, gives a time response in Fig. 4 with a steady-state amplitude of 0.14. Using the same initial displacement $U_0 = 0.95$ of the gap at $\delta = 0.05$, above the unstable branch, gives a time response in Fig. 5 with amplitudes greater than one, thus depicting the circular plate experiencing pull-in. The steady-state amplitudes obtained from the time responses in Figs. 4 and 5 are in perfect agreement with the bifurcation diagram Fig. 3. The voltage is kept constant for both time responses. So, the amplitude settles over time at the stable steady-state amplitude if any at that voltage. In the case of $\delta = 0.03$, which is at the left hand side of point B, the only stable steady-state amplitude is 0.14 of the gap on the lower branch (solid line). Therefore, although starting from an amplitude of 0.95 of the gap, the plate settles over time to the steady-state amplitude of 0.14 of the gap. In the case of $\delta = 0.05$, although there is a stable steady-state amplitude on the lower branch, because the plate starts from an amplitude of 0.95 of the gap which is above the unstable (dash line) branch AC, its amplitude will increase to pull-in.

Figures 6 and 7 illustrate the convergence of the ROM method using AUTO. ROM simulations show that seven terms are required for the ROM to predict the pull-in phenomenon from large amplitudes of a clamped circular plate. One can notice an excellent agreement between ROMs with $N = 2, 3, 4, 5, 6, 7$ terms up to amplitudes of 0.95 of the gap. However, above this point only 7T-ROM captures the behavior of the resonator plate showing no

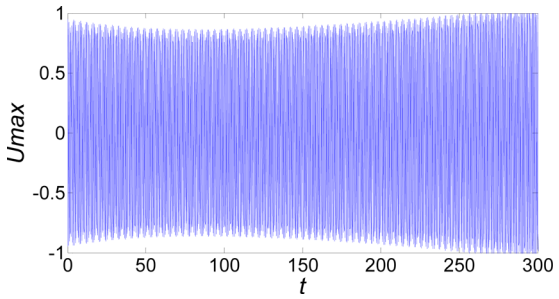

Fig. 5 Time response for MEMS clamped circular plate for 7T ROM, $\delta = 0.05$, $\mu = 0.005$, $\sigma = -0.005$, initial amplitude $U_0 = 0.95$

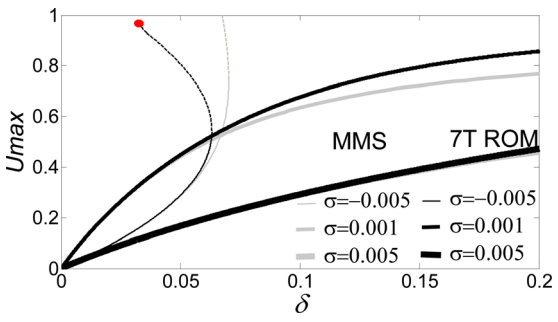

Fig. 8 Effect of frequency parameter σ on the voltage response for MEMS clamped circular plate using MMS and seven term ROM, $\mu = 0.005$

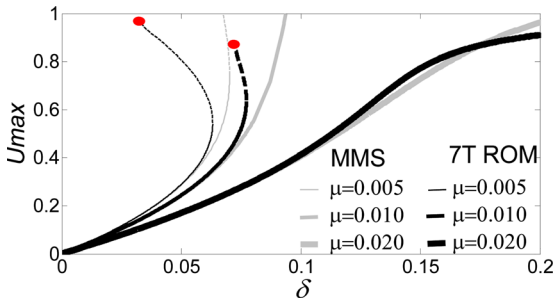

Fig. 9 Effect of damping parameter μ on the voltage response for MEMS clamped circular plate using MMS and seven term ROM, $\sigma = -0.005$

stable steady-state solutions, i.e., the unstable branch end at point B. This is clearly seen in Fig. 7.

Figure 8 shows the influence of the AC frequency on the voltage response of the system for three cases of frequency detuning parameter, $\sigma = -0.005$, $\sigma = 0.001$, and $\sigma = 0.005$ using 7T ROM and MMS. One can notice that as the frequency increases, the plate goes from a nonlinear behavior to a linear behavior. For $\sigma = 0.001$ and higher, the circular plate no longer experiences a bifurcation point or pull-in instability. When $\delta = 0.2$, the system reaches a maximum amplitude of $U_{\max} = 0.86$ for $\sigma = 0.001$ and $U_{\max} = 0.48$ for $\sigma = 0.005$. The results from MMS exhibit the same behavior. Results from MMS and 7T ROM are identical for low amplitudes. However, MMS fails to predict the nonlinear behavior at amplitudes larger than 0.4 of the gap.

Figure 9 shows the effect of the dimensionless damping parameter μ on the voltage–amplitude response at $\sigma = -0.005$. Starting from a low damping coefficient of $\mu = 0.005$, as the damping parameter increases, the curves for the response of the system shift from exhibiting nonlinear behavior to linear behavior. Also, a larger voltage is required to achieve the same amplitude of vibration if large damping. The voltage required to reach the bifurcation point, and therefore pull-in, increases as the damping of the system increases. Pull-in instability cannot be reached if $\mu = 0.020$ in the investigated range of voltage values. MMS is in perfect agreement with the results from 7T ROM for low amplitudes.

Discussion and Conclusions

The results of this investigation are obtained using analytical and numerical methods. The analytical solution is obtained using a perturbation method, namely, MMS. The system is numerically modeled using two, three, four, five, six, and seven term ROM to show the convergence of this method. It is found that seven terms ROM are necessary to accurately predict nonlinearities in the system such as the bifurcation points and pull-in phenomena. Time responses for different cases are obtained in order to find the steady-state amplitudes of vibration of the center of the plate. These steady-state amplitudes of vibration are in agreement with the results of the voltage–amplitude response obtained using AUTO 07P software [25] for seven terms ROM.

However, using MMS with one mode of vibration and Taylor expansions up to the third power of the nonlinear electrostatic forces, as in this work, fails to predict the nonlinearities of the system at higher amplitudes such as the bifurcation points and pull-in phenomenon. A remark is necessary. Since model order reduction is a technique to reduce complex models to an associated state-space dimension, i.e., a number of degrees of freedom, MMS is used to analytically solve one term (one mode of vibration) ROM since it uses only one mode of vibration, Eq. (15), while ROM with more than two terms are numerically integrated.

The voltage–amplitude response for the effects of detuning frequency and damping are reported. It is found that an increase in frequency and/or damping results in a shifting from nonlinear behavior to linear behavior. Recent work using ROM for MEMS cantilevers was reported in the literature [36].

Although MMS is an effective method to model the behavior of a clamped circular plate, it is limited to weak nonlinearities and cannot predict bifurcation points or pull-in of the system. It was found that such phenomena can be predicted using 7T ROM. Using a model with less terms would give results that show unrealistic behavior and incorrect prediction of pull-in instability.

A comparison between the voltage response of primary resonances of MEMS circular plates of this work and MEMS cantilevers reported in the literature [5] (both subjected to soft AC voltage of frequency near half natural frequency of the structure) shows a similar behavior of both structures. Moreover, the effects of frequency on the voltage response as well as damping are similar for both MEMS structures. One of the differences is that the saddle-node bifurcation point A for MEMS circular plates occurs at amplitudes slightly less than for MEMS cantilevers, although in the same range of 0.5–0.6 of the gap. Another difference is that the saddle-node bifurcation voltage parameter for MEMS circular plates is significantly higher than for MEMS cantilevers. Moreover, probably the most important difference is that the MEMS clamped circular plates do not have stable steady-state amplitudes close to the gap value as MEMS cantilevers have [5].

Although only AC voltage is considered since mass sensing applications are of interest, this work can be extended to a combined DC and AC voltage. The DC component in some cases can alter the bifurcation types [15]. This work can be extended to non-axisymmetric vibrations, higher natural frequencies, and experimental investigations.

Acknowledgment

This material is based on research sponsored by Air Force Research Laboratory under Agreement No. FA8650-07-2-5061. The views and conclusions contained herein are those of the authors and should not be interpreted as necessarily representing the official policies or endorsements, either expressed or implied, of Air Force Research Laboratory or the U.S. Government.

References

[1] Nayfeh, A. H., Abdel-Rahman, E., and Younis, M., 2003, "A Reduced-Order Model of Electrically Actuated Microbeam-Based MEMS," J. Microelectromech. Syst., **12**, pp. 672–680.
[2] Batra, R. C., Porfiri, M., and Spinello, D., 2008, "Reduced-Order Models for Microelectromechanical Rectangular and Circular Plates Incorporating the Casimir Force," Int. J. Solids Struct., **45**, pp. 3558–3583.
[3] Eoma, K., Park, H. S., Yoon, D. S., and Kwon, T., 2011, "Nanomechanical Resonators and Their Applications in Biological/Chemical Detection: Nanomechanics Principles," Phys. Rep., **503**, pp. 115–163.
[4] Desmaele, D., Boukallel, M., and Regnier, S., 2011, "Actuation Means for the Mechanical Stimulation of Living Cells Via Microelectromechanical Systems: A Critical Review," J. Biomech., **44**(8), pp. 1433–1446.
[5] Caruntu, D. I., Martinez, I., and Taylor, K., 2013, "Voltage-Amplitude Response of Alternating Current near Half Natural Frequency Electrostatically Actuated MEMS Resonators," Mech. Res. Commun., **52**, pp. 25–31.
[6] Ouakad, H., and Younis, M., 2010, "The Dynamic Behavior of MEMS Arch Resonators Actuated Electrically," Int. J. Non-Linear Mech., **45**(7), pp. 704–713.
[7] Abdel-Rahman, E., Nayfeh, A. H., and Younis, M., 2003 "Dynamics of an Electrically Actuated Resonant Microsensor," International Conference on MEMS, NANO and Smart Systems (ICMENS'03), July 20–23, pp. 188–196.
[8] Caruntu, D. I., Martinez, I., and Knecht, M. W., 2013, "Reduced Order Model Analysis of Frequency Response of Alternating Current Near Half Natural Frequency Electrostatically Actuated MEMS Cantilevers," ASME J. Comput. Nonlinear Dyn., **8**(3), p. 031011.
[9] Chen, J., Kang, S., Zou, J., Liu, C., and Schutt-Aine, J., 2004, "Reduced-Order Modeling of Weakly Nonlinear MEMS Devices With Taylor-Series Expansion and Arnoldi Approach," J. Microelectromech. Syst., **13**(3), pp. 441–451.
[10] Caruntu, D., and Martinez, I., 2014, "Reduced Order Model of Parametric Resonance of Electrostatically Actuated MEMS Cantilever Resonators," Int. J. Non-Linear Mech., **66**, pp. 28–32.
[11] Saleem, F., and Younis, M., 2009, "Controlling Dynamic Pull-In Escape in Electrostatic MEMS," International Symposium on Mechatronics and its Applications (ISMA09), Sharjah, UAE, Mar. 23–26.
[12] Ghayesh, M., Farokhi, H., and Amabili, M., 2013, "Nonlinear Behavior of Electrically Actuated MEMS Resonators," Int. J. Eng. Sci., **71**, pp. 137–155.

[13] Lee, W., and Yeo, M., 2003, "Non-Linear Interactions in Asymmetric Vibrations of a Circular Plate," J. Sound Vib., **263**(5), pp. 1017–1030.
[14] Caruntu, D. I., and Knecht, M. W., 2011, "On Nonlinear Response Near Half Natural Frequency of Electrostatically Actuated Microresonators," Int. J. Struct. Stability Dyn., **11**(4), pp. 641–672.
[15] Caruntu, D. I., and Taylor, K. N., 2014, "Bifurcation Type Change of AC Electrostatically Actuated MEMS Resonators Due to DC Voltage," Shock Vibration, **2014**, p. 542023.
[16] Liao, L.-D. L., Chao, P. C.-P., Huang, C.-W., and Chiu, C.-W., 2010, "DC Dynamic and Static Pull-In Predictions and Analysis for Electrostatically Actuated Clamped Circular Micro-Plates Based on a Continuous Model," J. Micromech. Microeng., **20**(2), p. 025013.
[17] Wang, Y.-G., Lin, W.-H., Li, X.-M., and Feng, Z.-J., 2011, "Bending and Vibration of an Electrostatically Actuated Circular Microplate in Presence of Casimir Force," Appl. Math. Modell., **35**(5), pp. 2348–2357.
[18] Ahmad, B., and Pratap, R., 2010, "Elasto-Electrostatic Analysis of Circular Microplates Used in Capacitive Micromachined Ultrasonic Transducers," IEEE Sens. J., **10**(11), pp. 1767–1773.
[19] Sharafkhani, N., Rezazadeh, G., and Shabani, R., 2012, "Study of Mechanical Behavior of Circular FGM Micro-Plates Under Nonlinear Electrostatic and Mechanical Shock Loadings," Acta Mech., **223**(3), pp. 579–591.
[20] Ansari, N., Gholami, R., Faghih Shojaei, M., Mohammadi, V., and Sahmani, S., 2014, "Surface Stress Effect on the Pull-In Instability of Circular Nanoplates," Acta Astronaut., **102**, pp. 140–150.
[21] Rashvand, K., Rezazadeh, G., Mobki, H., and Ghayesh, M. H., 2013, "On the Size-Dependent Behavior of a Capacitive Circular Micro-Plate Considering the Variable Length-Scale Parameter," Int. J. Mech. Sci., **77**, pp. 333–342.
[22] Zhang, W.-M., Yan, H., Peng, Z.-K., and Meng, G., 2014, "Electrostatic Pull-In Instability in MEMS/NEMS: A Review," Sens. Actuators A, **214**, pp. 187–218.
[23] Vogl, G., and Nayfeh, A. H., 2005, "A Reduced-Order Model for Electrically Actuated Clamped Circular Plates," J. Micromech. Microeng., **15**(4), pp. 684–690.
[24] Caruntu, D. I., Martinez, I., and Knecht, M. W., 2015, "Parametric Resonance Voltage Response of Electrostatically Actuated Micro-Electro-Mechanical Systems Cantilever Resonators," J. Sound Vib., **362**, pp. 203–213.
[25] Doedel, E. J., and Oldeman, B. E., 2009, *AUTO-07P: Continuation and Bifurcation Software for Ordinary Differential Equations*, Concordia University, Montreal, QC, Canada.
[26] Pelesko, J. A., and Bernstein, D. H., 2003, *Modeling MEMS and NEMS*, Chapman & CRC Hall/CRC, Boca Raton, FL.
[27] Banks-Sills, L., Hikri, Y., Krylov, S., Fourman, V., Gerson, Y., and Bruck, H. A., 2011, "Measurement of Poisson's Ratio by Means of a Direct Tension Test on Micron-Sized Specimens," Sens. Actuators A, **169**(1), pp. 98–114.
[28] Younis, M. I., and Nayfeh, A. H., 2003, "A Study of the Nonlinear Response of a Resonant Microbeam to Electric Actuation," Nonlinear Dyn., **31**(1), pp. 91–117.
[29] Nayfeh, A. H., 1981, *Introduction to Perturbation Techniques*, Wiley, New York.
[30] Nayfeh, A. H., and Mook, D. T., 1979, *Nonlinear Oscillations*, Wiley, New York.
[31] Rao, S. S., 2007, *Vibration of Continuous Systems*, Wiley, Hoboken, NJ.
[32] Leissa, A. W., 1969, "Vibration of Plates," NASA SP-160.
[33] Younis, M. I., Ouakad, H. M., Alsaleem, F. M., Miles, R., and Cui, W., 2010, "Nonlinear Dynamics of MEMS Arches Under Harmonic Electrostatic Actuation," J. Microelectromech. Syst., **19**(3), pp. 647–656.
[34] Ibrahim, M. I., and Younis, M. I., 2010, "The Dynamic Response of Electrostatically Driven Resonators Under Mechanical Shock," J. Micromech. Microeng., **20**(2), p. 025006.
[35] Lakrad, M., and Belhaq, M., 2011, "Suppression of Pull-In in a Microstructure Actuated by Mechanical Shocks and Electrostatic Forces," Int. J. Non-Linear Mech., **46**(2), pp. 407–414.
[36] Caruntu, D. I., and Knecht, M., 2015, "MEMS Cantilever Resonators Under Soft AC Voltage of Frequency Near Natural Frequency," ASME J. Dyn. Syst., Meas. Control, **137**(4), p. 041016.